Dielectric Relaxation Studies of Water-Containing Short Side Chain Perfluorosulfonic Acid Membranes

Z. D. Deng and K. A. Mauritz*

Department of Polymer Science, University of Southern Mississippi, Southern Station Box 10076, Hattiesburg, Mississippi 39406-0076

Received August 29, 1991

ABSTRACT: The storage and loss components of the complex dielectric permittivities of short side chain perfluorosulfonic acid membranes were determined as a function of water content, temperature, and membrane equivalent weight. As in our previous studies of electrolyte-containing long and short side chain perfluorosulfonate ionomers, a low-frequency graphical feature on isothermal loss spectra was identified that is suggested to be reflective of, and that crudely quantifies the tortuousity of, long-range (intercluster) proton-conductive pathways. When the long-range ion transport contribution was subtracted from the loss spectra, a distinct bimodal relaxation was uncovered. It is suggested that these two relaxation peaks are a manifestation of two distinct types of hydrated polar clusters. At least one of the peaks is assumed to arise from a cluster/TFE interfacial polarization that fluctuates with a characteristic frequency as indicated by the maximum loss factor. Finally, preliminary studies suggest that the Cole–Cole distribution of relaxation times parameter for nominally dry membranes may be an index of distribution of cluster size or of cluster structure.

Introduction

Perfluorinated ionomer membranes have received considerable attention in vital areas dealing with the production of industrial chemicals and the generation of electrical energy, mainly as ion-permselective separators in electrochemical processes. Long side chain perfluorosulfonate ionomer (PFSI) membranes were developed by the E. I. Du Pont Co. under the trade name Nafion, and its chemical structure is shown in Figure 1. Mauritz and co-workers have extensively characterized the dynamic ionic-hydration microstructures of these long side chain PFSIs using FT-IR, solid-state multinuclear NMR, and dielectric relaxation spectroscopies, mainly. It is widely accepted that there exists in these ionomers a somewhat ill-defined hydrophilic/hydrophobic microphase separation in the form of sulfonate-rich clusters that are nanometers in size and that these clusters are embedded in a highly crystalline perfluorocarbon matrix. An extensive documentation of these studies is included in ref 1 or in the references enumerated in this paper.

The Dow Chemical Co. has also developed a similar but shorter side chained PFSI whose structure is also displayed in Figure 1. Tant et al.,[2] on the basis of dynamic mechanical relaxation, DSC, and WAXD studies, reported that the short side chain materials exhibit two types of crystallinity and, on a comparative basis, display higher T_gs than their long side chain counterparts. The T_g for the Na^+ form was higher than that for the acid form for a given equivalent weight (EW), indicating greater interactive cohesion within the ionic form. The short side chain PFSIs are also considered to possess a polar/nonpolar microphase separation as well as a TFE-like crystallinity, as independently reported by Moore and Martin, based on their SAXS, WAXD, and DSC investigations.[3]

In a number of papers by Mauritz et al., all of which are listed in ref 1, it was pointed out how the dielectric relaxation spectra of both the long and short side chain PFSI membranes, which contained various aqueous electrolyte solutions of different concentrations, displayed characteristics that were reflective of both the long- and short-range motions of hydrated ions throughout the heterophase morphologies of these systems. As we have provided an in-depth rationalization of our interpretation of the spectra for these systems in these papers, we only offer a synopsis of the salient concepts below.

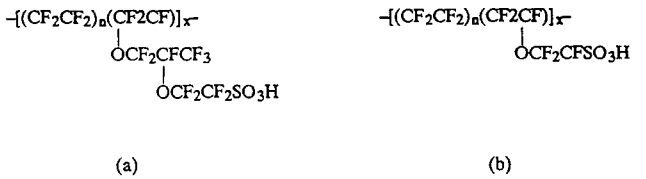

Figure 1. Chemical structures of the (a) long side chain (Nafion) and (b) short side chain (Dow) perfluorosulfonate ionomers in the acid forms.

Long-range ion displacements are manifest by a distinct linear segment in the low-frequency region of log ϵ'' vs log f plots, where ϵ'' is the dielectric loss factor and f is the frequency of the (weak) electric field applied via an impedance analyzer. The loss spectra for all electrolyte-imbibed PFSI membrane systems investigated to date can be expressed very well as a linear superposition of two terms

$$\epsilon'' = \epsilon_{ac}'' + A\omega^{-n} \tag{1}$$

where $\omega = 2\pi f$, A is a curve-fitted constant for a given membrane–electrolyte system, and n is the fitted slope of the linear section of the curve. We have reasoned that the parameter n is a coarse morphological index in the sense that it is a reflection of the overall *connectivity* of the macroscopic ensemble of ionic clusters in a given membrane state. The obvious disorder that must exist in the three-dimensional packing of clusters is expected to produce dead ends or ion traps that are distributed more or less randomly over the conductivity grid. The lower the value of n, the greater is the degree of this intercluster disorder. This concept is roughly illustrated in Figure 2. In other words, as n decreases, the long-range ion conductive pathways, on the average, become more tortuous. We have, in fact, expressed the view that long-range ion hopping within these systems might be appropriately viewed as a process that is *fractal* in space, or in time, or in both. There are two special mechanistic assignments that represent distinct, familiar processes: $n = 1$, which corresponds to pure unidirectional ion migration, or "drift"; $n = 1/2$ which represents pure diffusion, that is, random ionic walks.

The ϵ_{ac}'' term in eq 1 represents often obscured high-frequency relaxation peaks that are superimposed on the

0024-9297/92/2225-2739$03.00/0

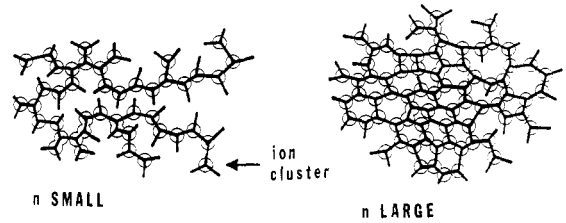

Figure 2. Crude depiction of networks of ionic clusters that are poorly (left) and highly (right) interconnected with respect to ion hopping between adjacent clusters.

overwhelming long-range component of the spectrum. ϵ_{ac}'' vs ω peaks are in practice resolved from the total spectrum by the point-by-point subtraction of fitted $A\omega^{-n}$ values from the corresponding "total" ϵ'' values over the high-frequency range. This relaxation has been mechanistically attributed to *intra*cluster ion motions which are envisioned as follows. The relaxation time, $\tau = \omega_{max}^{-1}$, is associated with the natural time scale during which the alternate accumulation and dissipation of ionic charge occurs, due to thermal fluctuations, at the hydrophilic/hydrophobic phase boundaries in cooperative fashion. This *relaxation of interfacial polarization*, in turn, arises owing to the gradients of ionic mobilities across these interfaces. Given this interpretation, τ is expected to be, and in fact is observed to be, quite sensitive to the concentrations of cluster-contained mobile ions. This ionic concentration dependence is reasonably attributed to the progressive association of cluster-incorporated ions into electrically neutral pairs and motionally sluggish higher-order multipoles, with increasing concentration. It was suggested that the width, or a possible multicomponent status of this peak, might signal a distribution of cluster *types*. It was also suggested that the enormous observed values of ϵ_0, the zero-frequency limit of ϵ', are due to the magnitude of this interfacial polarizibility mechanism.

Our recent dielectric relaxation analysis of aqueous H_2SO_4-containing short side chain PFSI membranes has uncovered all of the above-mentioned spectral features.[1] A simple equivalent circuit permittivity model and its mathematical representation were proposed for this system. The success of the mathematical model reinforces our usual formal decomposition of the relaxation spectra into two basic contributions associated with the intercluster and intracluster motions of ions throughout the clustered morphology. The organized response of the parameters n and τ to acid concentration and temperature were observed, and the reader is referred to ref 1 for the numerous details and conclusions of this study. We will make comparisons between these previous results and the results of the present study where appropriate. A particularly interesting outcome of these studies is the appearance of a bimodal high-frequency relaxation peak, at the lowest acid concentration (similarly assigned to a fluctuating interfacial polarization), that suggests the existence of two types of ion clusters at high water contents.

In the studies reported herein, the dielectric relaxation spectra of short chain PFSI membranes incorporating controlled levels of pure water were obtained. While neither mobile counterions nor co-ions are present in these membranes, the hydrated protons will possess great mobility owing to the levels of hydration as well as to the very low pK_a of the sulfonic acid groups.

Experimental Section

PFSI membranes of 795, 964, and 1001 EW were processed and supplied by the Dow Chemical Co. through the efforts of C. W. Martin. All membranes, having a nominal thickness of about 0.18 mm, were systematically initialized using the following standard procedure before the water uptake was affected. First, the membranes were equilibrated in 14 M H_2SO_4 solutions for 48 h to ensure the conversion of all of the fixed sulfonate groups to the desired acid form. Then, the films were soaked in deionized water for 48 h to leach out the excess H_2SO_4 component. At this point, the samples are considerably swollen with water and the H^+:SO_3^- mole ratio is 1. Having been dried at 100 °C under vacuum for 48 h, the membranes were stored in a desiccator until the controlled uptake of water was affected. This standard membrane initialization protocol was uniformly applied to ensure that all samples entered experimentation in the same chemical state and having experienced the same swelling and thermal histories.

Table I
Percent Weight Increase and Average Number of Water Molecules per Sulfonic Acid Group for Initially Dry Short Side Chain PFSI Membranes, of Indicated Equivalent Weights, That Were Equilibrated in Pure Water

EW	wt gain, %	H_2O/SO_3^-
795	34	15.2
964	18	9.7
1001	19	10.6

Prior to the impedance measurements, the initialized membranes were imparted various degrees of hydration by the following method.

The dried membranes were soaked in pure deionized water, at room temperature, for at least 48 h to saturation. The hydrated membranes were then surface blotted dry before being put into a parallel plate electrode test cell, and the electrical impedance measurements were taken over the frequency range 5 Hz–10 MHz using an HP 4192A LF impedance analyzer controlled by a PC through a GPIB. The applied sinusoidal voltage signal had an rms amplitude of only 5 mV so that the electrical response can be expected to be linear, as desired. The impedance data were corrected for the contribution from the empty cell. The raw impedance data were later converted to the real (storage) and imaginary (loss) components of the complex dielectric permittivity, $\epsilon^* = \epsilon' - i\epsilon''$, at each tested frequency using the equation[1]

$$\epsilon^* = l/(i\omega\epsilon_0 A_c Z^*) \qquad (2)$$

where $i = -1^{1/2}$, ϵ_0 is the known dielectric permittivity of free space, A_c is the electrode surface area, l is the membrane thickness, and Z^* is the measured electrical impedance. All impedance experiments were performed inside a constant-humidity chamber to avoid any possible evaporation of water from the membranes.

The membranes were weighed before and after hydration, and the percent weight uptakes at water saturation are listed in Table I. It is seen that the 795 EW sample has a considerably higher water uptake than that of each of the other two samples. This outcome is consistent with the simple fact that lower EW membranes contain more fixed sites for hydration. The difference between the uptakes of the 964 and 1001 EW films is actually so small as to be within experimental error. The two EW values, as measured, are considered to be very close to each other. There is a probable error of about 20 units in the determination of equivalent weight by titration (source: Dow Chemical Co.). It should also be mentioned that the stated EW should be an average over a microscopic (albeit unknown) distribution. Also, the average number of incorporated water molecules per SO_3H group was calculated and is listed in Table I for each EW. Given the fact that this ratio is rather high in all cases and that SO_3H is a very strong acid group, the protons within these membranes can be expected to be mainly dissociated from the sulfonate groups and highly mobile, being able to hop with great facility across numerous hydrogen bonds within the hydration microstructure. Our infrared spectroscopic investigations of acid-form PFSI systems indicate that most of the imbibed water is in fact free (i.e., hydrogen bonded) rather than strongly ion bound.[4] Our subsequent analysis of the dielectric relaxation results will depend in part on these simple but important facts.

Partially hydrated membranes were produced by allowing fully hydrated samples to equilibrate in atmospheres of different

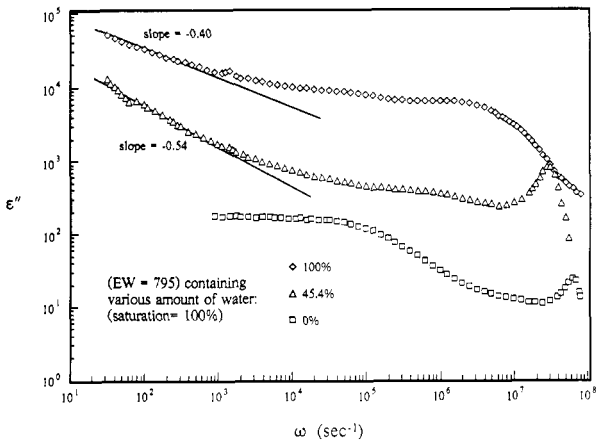

Figure 3. ϵ'' vs ω for 795 EW membranes having indicated water contents at 22 °C.

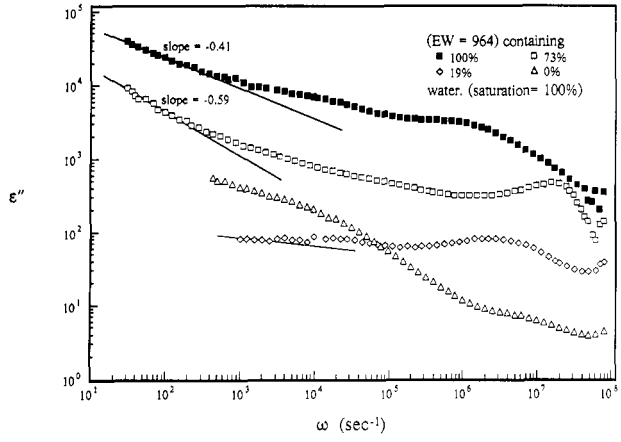

Figure 4. Same as Figure 3 but for EW = 964.

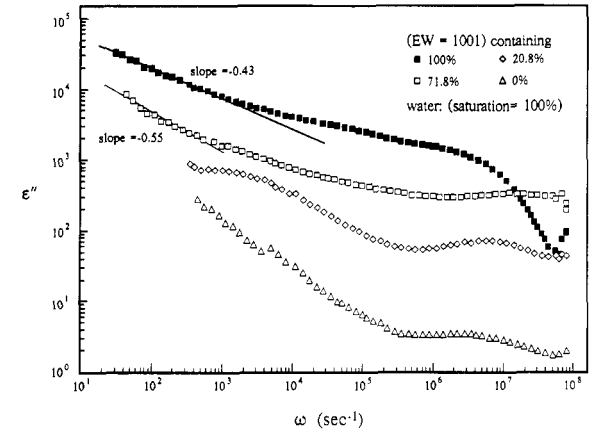

Figure 5. Same as Figure 3 but for EW = 1001.

relative humidities for 24 h. The weight changes of these membranes were measured and their dielectric relaxation spectra obtained.

Results and Discussion

Figures 3–5 show the dielectric loss spectra for the three EWs at the indicated degrees of hydration. "Degree of hydration", here, is defined so that 100% corresponds to water saturation, that is, the mass percent of the equilibrium uptake, or hydration capacity, without reference to the dry mass of the membrane. The water content in terms of the $H_2O:SO_3^-$ ratio is easily obtained using Table I. Of course, in the absence of established water vapor pressure–sorption isotherms for each EW, the exact degree of hydration cannot be predicted a priori. It is seen from

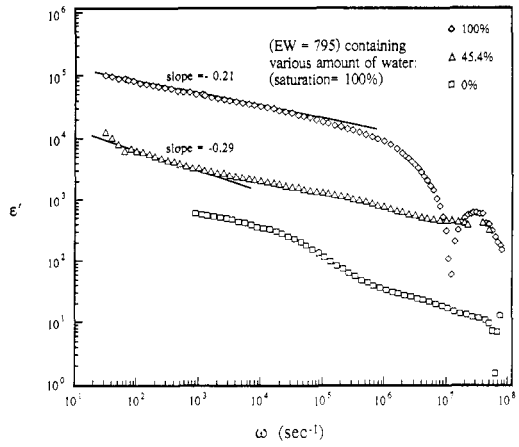

Figure 6. ϵ' vs ω for 795 EW membranes having indicated water contents at 22 °C.

Figures 3–5 that, on the whole, the curves are progressively shifted upward with increasing water content, the net shift amounting to almost 3 orders of magnitude. As these loss curves are obviously dominated by long-range ion transport, and increasingly so at lower frequencies, it is not difficult to imagine that the monotonic upward shift in ϵ'' at a given ω is due to an increasing protonic mobility with increasing degree of hydration for a given EW. In short, a greater number of hydrogen-bonded water molecules relative to protons increases the number of proton hopping possibilities which, in turn, translates into an enhanced intrinsic proton mobility. We would like to call attention to the fact that, in our previous studies of aqueous H_2SO_4-containing short side chain PFSI membranes, the loss curves at 22 °C shifted upward in the same fashion with decreasing acid concentration.[1] While the earlier situation is more complicated by the incorporation of the excess acid components, the decrease in concentration nonetheless corresponds to an increase in hydration.

One view might consider the progressive invasion of water throughout the membrane as inducing a greater degree of cluster ion-hopping interconnectivity. On the other hand, we note that for curves for which a slope $(-n)$ in the low-frequency region can be reasonably defined, n decreases as the degree of hydration increases. This trend generally also holds for the sulfuric acid-containing membranes as the concentration decreases, as seen in our earlier investigation.[1] As in the former studies, we suggest that as membrane dehydration proceeds the clusters shrink and pack more efficiently and that this, in turn, causes the ion-hopping interconnectivity of the clusters to increase.

It is also worthy to note that, for a given EW, the values of n are generally smaller than those displayed by the aqueous H_2SO_4-containing membranes. Of course, the acid-imbibed membranes are unable to incorporate more water than the corresponding pure water-containing membranes, the reason being that the water activity in the acid solutions will always be less than 1, the value for pure water. This comparison between water and acid-containing membranes reinforces the above-stated view that n decreases with increasing hydration level. It is of significant note that n values are 0.5 ± 0.1; that is, they do not vary greatly above and below the diffusion-associated value.

It can also be seen in Figures 3–5 that there is a high-frequency relaxation peak that can be resolved from the spectrum as described earlier.

Figures 6–8 consist of the dielectric storage spectra for the three EWs at the specified degrees of hydration. As

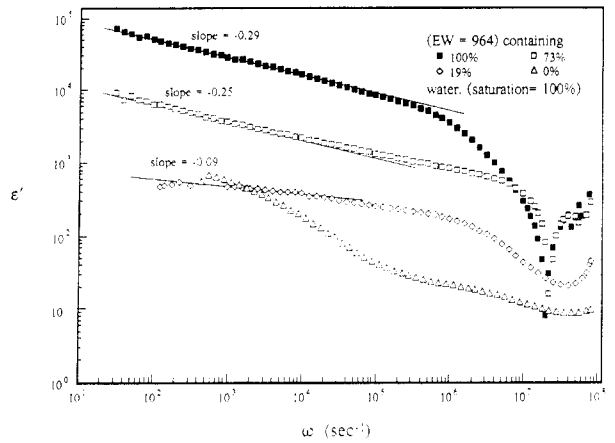

Figure 7. Same as Figure 6 but for EW = 964.

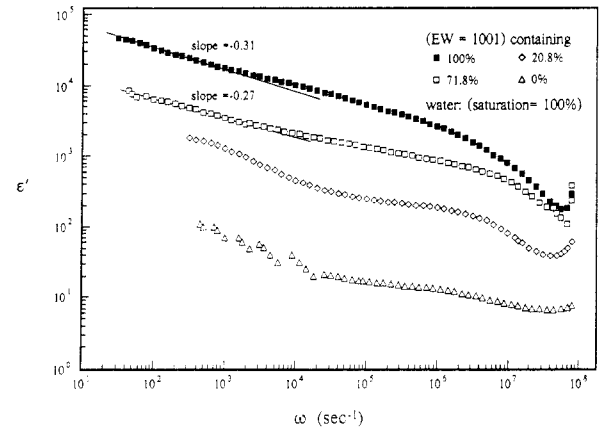

Figure 8. Same as Figure 6 but for EW = 1001.

Table II
Slopes of Low-Frequency Linear Segments of log ϵ' and log ϵ'' vs log ω Plots for Membranes of Listed Equivalent Weights Having Indicated Water Contents

EW	slopes at low frequencies	
	ϵ'	ϵ''
795	−0.21 (100%)	−0.40 (100%)
	−0.29 (45.4%)	−0.54 (45.4%)
964	−0.29 (100%)	−0.41 (100%)
	−0.25 (73%)	−0.59 (73%)
1001	−0.31 (100%)	−0.43 (100%)
	−0.27 (71.8%)	−0.55 (71.8%)

with the loss spectra, the curves are monotonically shifted upward with increasing water content. The vertical separation of the curves, on the whole, is profound, being about 2 orders of magnitude of ϵ' between the 0% and 100% curves. Furthermore, the back-extrapolated values of ϵ' (i.e., ϵ_0) are enormous, indicating great material polarizability. As progressively more water is incorporated within the membrane of a given EW, one might think that the relative amount of hydrophilic/hydrophobic interface increases. Recall that, in our view, net nonzero ionic charge periodically accumulates at these interfaces. Moreover, the mobility of cluster protons is enhanced in the manner as discussed earlier. Hydrated protons, therefore, with their increased mobility will migrate to the interface with greater facility and thereby increase the degree of accumulation of charge at the interfaces. By these two interrelated mechanisms, the degree of interfacial polarization would necessarily rise with increasing water content.

Last, we observe that the slopes of the low-frequency linear ϵ' vs ω curve segments, where discernible, are rather

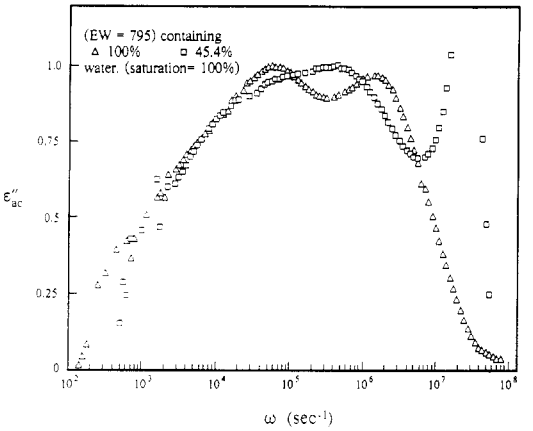

Figure 9. Curve-resolved ϵ_{ac}'' vs ω for 795 EW membranes having indicated water contents at 22 °C.

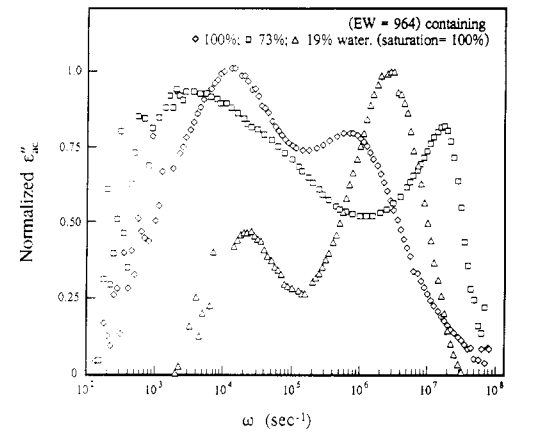

Figure 10. Same as Figure 9 but for EW = 964.

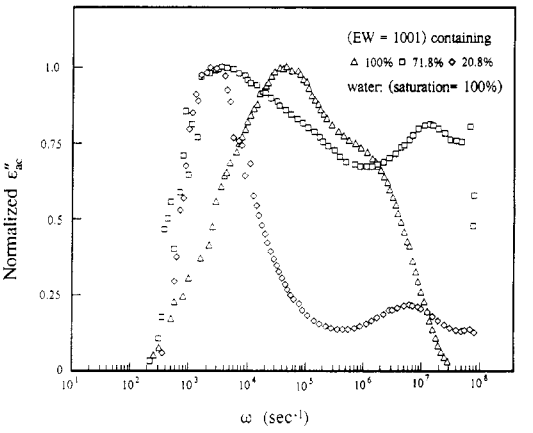

Figure 11. Same as Figure 9 but for EW = 1001.

low. It was earlier pointed out that values of n as derived from the corresponding loss curves are also low. Table II consists of a summary of the linear slopes for both the loss and storage spectra for the three EWs at the indicated water levels for the purpose of their intercomparison. It needs to be stated that the slopes for the storage curves are actually considerably lower in value than the slopes for the loss curves, so much so as to not be considered as being diffusion or Warburg component related. A reconciliation of this contrast is obviously needed.

The resolved ϵ_{ac}'' vs ω curves revealed two distinct and widely separated relaxation peaks at all water contents and for all three EWs, as seen in Figures 9–11. The low-frequency region peaks are generally in the range 10^3–10^4 s^{-1}, while the high-frequency region peaks are in the range 10^5–10^7 s^{-1}. It might be considered that the two peaks

represent two different relaxation processes because of their coexistence at two greatly different motional time scales. Perhaps the lower frequency peak could be identified with the aforementioned relaxation of interfacial polarization mechanism, being closest to the same frequency range as the similar relaxation observed for the aqueous H_2SO_4-containing membranes.[1] At this point, it is important to be reminded of the strong shoulder that appears on the high-frequency side of the relaxation peak for the membrane containing the lowest acid concentration in this prior study. We had earlier advanced the idea that the two peaks might represent two distinct *types* of hydrated cluster microstructures that are possible given a liberal quantity of sorbed water. In speaking of cluster "type" we are referring to the size, shape, and chemical composition of and structure within a cluster in a rather general way. Furthermore, protons would also conceivably have different mobilities in different types of clusters. To be sure, further refinement of this hypothesis would be imprudent, given the paucity of evidence, to date.

Let us now inspect Figures 9–11 in greater detail. For EW = 795 (Figure 9), both the high- and low-frequency peaks shift to the left as the water content increases from 45% to 100%. As before, one might say that the motional time scales within each of the two distinct hydration microstructures lengthen with increasing water content. Perhaps this behavior is due to a decrease in intracluster proton mobility with increasing cluster water content. Perhaps it should be interjected here that the actual *widths* of these peaks are proportional to $\Delta\omega/\omega_{max}$ owing to the use of a logarithmic frequency axis. For example, peaks at high frequencies may appear to be narrow on a logarithmic scale but are in effect compressed because differences in orders of magnitude represent much larger differences in frequency than do differences in orders of magnitude at low frequencies.

At EW = 964 (Figure 10), neither the high- nor the low-frequency peak seems to exhibit a shift pattern with increasing water content, although more hydration levels should probably be inspected before conclusions are reached in regard to trend. It is noted that the peak separation is greatest at the intermediate water content.

At EW = 1001 (Figure 11), it is seen that both the low- and high-frequency peak positions do not shift significantly from 21% to 72% water content. On the other hand, at water saturation, the two peaks are closer to each other, which might indicate that the hydration microstructure is becoming more homogeneous. Recall that the 1001 EW membrane will have the lowest equilibrium water content of the three.

Further insight into the nature of the high-frequency relaxation can be obtained by inspecting the dielectric response of *dry* sulfonic acid form membranes. For truly dry systems, the overwhelming obscuration of short-ranged relaxations by long-range transport effects that extend over the spectrum is hypothetically minimal. To be sure, it is well understood that membranes of this sort are difficult to dry down to the last water molecule. Add to this the strong acid nature of the SO_3H group in this perfluorinated chemical environment, and it is not difficult to understand that residual mobile protons will still be present in conventionally "dried" membranes and that these charge carriers might be detected as executing long-range motions in the dielectric spectra.

While we have been representing dielectric relaxation results for PFSI membranes in terms of ϵ' vs ω and ϵ'' vs ω plots, both long- and short-range ion motions also manifest themselves as distinct understandable features on Cole–Cole plots, i.e., ϵ'' vs ϵ' over the tested frequency range. The Cole–Cole plots for the three equivalent weight membranes in the dry sulfonic acid form are displayed in Figures 12–14. As usual, the points correspond to increasingly higher applied signal frequency in passing from right to left. Therefore, the time scales at which observed relaxation processes occur decrease in this order. Semicircles are usually indicative of motions that are confined

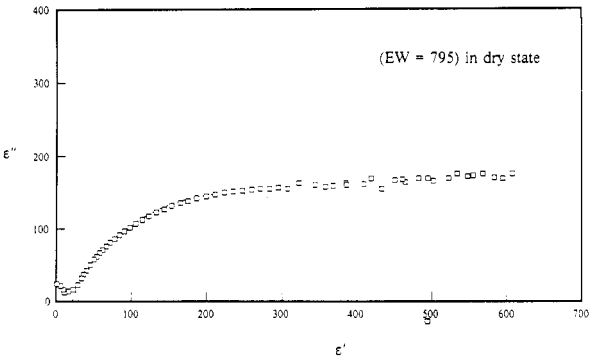

Figure 12. Cole–Cole plot for 795 EW membrane in the dry state. Also plotted are the fitted semicircle and associated center point.

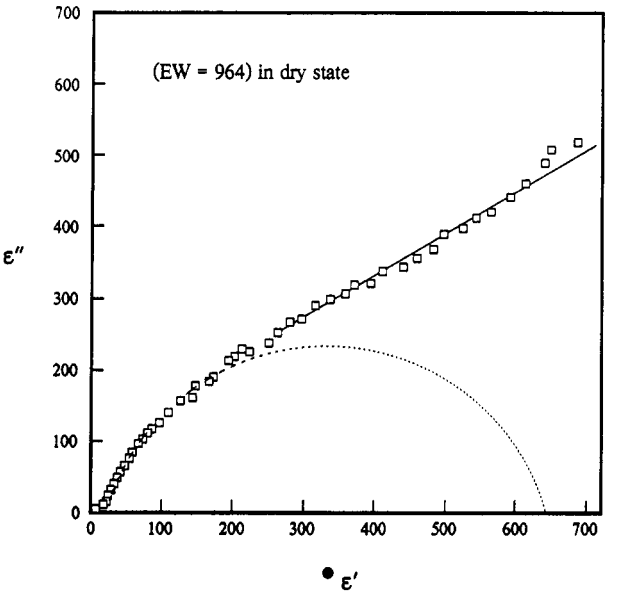

Figure 13. Same as Figure 12 but for 964 EW membranes.

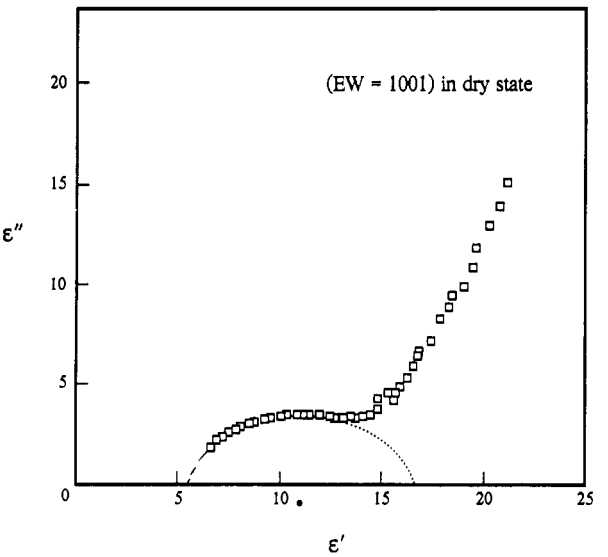

Figure 14. Same as Figure 12 but for 1001 EW membranes.

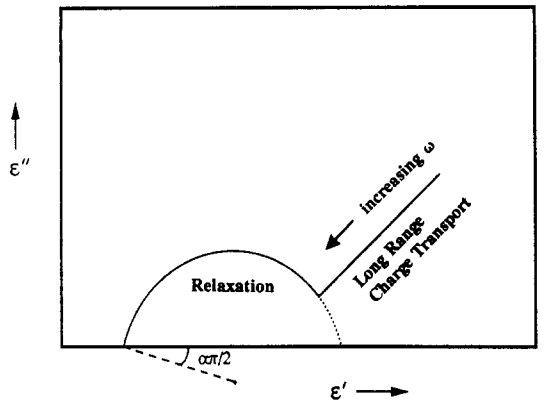

Figure 15. Hypothetical Cole–Cole plot for a system having (1) a single relaxation with a distribution of relaxation times characterized by the parameter α and (2) long-range charge transport represented by the linear segment at low frequencies.

within a characteristic region of space. Examples of this sort of relaxation would be dipole reorientation of a single molecule in a mean field (as in a polar liquid as described by the original theory of Debye), the cooperative (coupled) motions of polymer chain-attached dipoles, or a fluctuating interfacial polarization occurring in the region of, say, a nanometers in size morphological feature (e.g., ion cluster in a medium of low dielectric constant). We have demonstrated that long-range ion motions, which in our system would effectively involve an electrode plate-to-plate transfer of mobile ions at zero applied frequency are characterized by a monotonically decreasing behavior of not only ϵ' but also ϵ'', with increasing frequency. Therefore, if both ϵ' and ϵ'' have a power law decrease with increasing frequency, long-range ion motions on a Cole–Cole plot will appear as straight lines in the right-hand portion of the plot, and these lines will merge to the left with a relaxation semicircle, as ideally depicted in Figure 15.

At the higher frequencies the points in Figures 12–14 can be very well fitted to a semicircle whose center is depressed beneath the ϵ' axis. This feature, in our interpretation, corresponds to the relaxation of polarization at the hydrophilic/hydrophobic (cluster/TFE) interfaces. One of the advantages of representing dielectric relaxation data in this way is the ability to extract not only relaxation times but their distributions about most probable values. The familiar Cole–Cole distribution of relaxation times parameter, α, is obtained by measuring the angle between the horizontal ϵ' axis and the radius that passes through the intersection of the circular arc with the ϵ' axis as illustrated in Figure 15.[5] An increase in α, that is, a depression of the semicircle, is interpreted in terms of an increase in microstructural heterogeneity. "Heterogeneity", in general, usually refers to either a natural distribution of the immediate molecular level environment about the relaxing structural unit or a distribution of the structure of the relaxing unit itself. In terms of the system at hand, and given our previous assignment of this relaxation, we view α as being reflective of the distribution of cluster type, as discussed previously.

Perhaps this is the most logical place in our discussion to point out that we have now identified parameters that can be extracted from the dielectric relaxation spectra of PFSI membranes that are indicative of morphological regularity on both the long- and short-range structural levels (i.e., n, as relating to *inter*cluster, and α, as relating to *intra*cluster order).

If α is extracted in this way from the Cole–Cole plots in Figures 12–14, the following monotonic progression with EW is revealed: α = 0.11 (1001 EW), 0.18 (964 EW), 0.23 (795 EW). Obviously, it would be better to have α values for a greater number of different membrane EWs in hand before definite conclusions regarding trends in this quantity are reached. Furthermore, it was earlier pointed out that the difference between the 964 and 1001 EW membranes is not very great. On the other hand, it would be of considerable interest to see if dielectric relaxation analysis in fact has the sensitivity to adequately discriminate between membranes having EWs that do not differ by this much. Clearly, this is an important subject for future exploration. Therefore, these results only tentatively suggest that the distribution of cluster structures broadens with decreasing EW. Perhaps this conclusion is quite reasonable, considering that an increased number of cluster structural possibilities would exist at lower equivalent weights owing to a greater number of side chains that would be available to form aggregates of various sizes. In terms of theoretical models of the aggregation of polymer-attached polar groups, most notably that of Forsman,[6] one might think in terms of low EW ionomers as having more available ways of distributing chain-attached ion dipoles throughout a macroscopic ensemble of nanometer in size polar aggregates. Having a distribution of cluster sizes would be an entropy-satisfying process in superimposing a measure of disorder on the energy-driven process of ionic cluster formation. It should also be remembered that the crystalline order associated with the packing of TFE chains in the hydrophobic intercluster regions will also be progressively disrupted with decreasing EW. This latter factor might in fact conspire with the former to cause α to increase with decreasing EW. At this time we are merely offering these ideas as a hypothetical framework upon which further definitive experimentation can be based.

Finally, the linear departures from and to the right of the depressed semicircles are assigned to intercluster ion hopping, as earlier discussed. While we presently feel that the slope of the linear segment of a log ϵ'' vs log ω plot has a definite interpretation within an albeit crude theoretical framework, the meaning of a slope of a linear segment on a Cole–Cole plot is more ubiquitous, mainly because dielectric storage (polarization) effects are superimposed upon dielectric loss effects.

General Conclusions

We have performed a detailed dielectric relaxation analysis of pure H_2O-containing short side chain perfluorosulfonic acid membranes as a function of equivalent weight, water content, and temperature. The following distinct fingerprints of long- and short-range proton transport and ionomer microstructure were identified in the relaxation spectra.

(1) Extremely high dielectric storage factors (ϵ') that would seem to arise from considerable interfacial polarization reflect the known hydrophilic/hydrophobic microphase separation in these ionomers.

(2) The occurrence of linear segments in the low-frequency region of all log ϵ'' vs log ω plots is a clear signature of long-range, i.e., intercluster, ion transport. The slopes of these lines ($-n$) are a measure of the degree to which long-range ion displacements are controlled by ionic drift (n = 1), by diffusion (n = $^1/_2$), or by a hybrid, less clearly defined transport situation. In terms of polymer morphology, n is a coarse measure of the degree of ion transport connectivity over a large array of ionic clusters such that migration pathways become more tortuous with decreasing n. A system with low n has ion

conductive pathways that are not highly interconnected and contain dead ends, i.e., charge traps. Therefore, one might conjecture that methods of membrane synthesis or processing, or subsequent chemical or physical modifications that result in a more homogeneous microstructure, i.e., procedures that lead to systems with high n values, would be beneficial. We discussed a number of modifications that might serve to control n in our previous paper.[1]

(3) In a number of instances, the vertical shifting of ϵ' and ϵ'' vs ω curves, either as a function of water concentration at constant temperature, or as a function of temperature at constant water concentration, is rationalized in terms of electrostatically bound associations of ions within cluster microsolutions.

(4) Relaxation maxima appear in the high-frequency region of the dielectric loss spectra. These peaks were resolved from the ϵ'' vs ω curves by the point-by-point subtraction of the long-range-associated loss component, which is proportional to ω^{-n}, from ϵ'' in the high-frequency spectral region. This discrete relaxation is believed to be of an intracluster nature and to arise from the alternate accumulation and dissipation of net ionic charge at the hydrophobic/hydrophilic phase boundaries during a half cycle of applied electric field oscillation. In short, the relaxation times derived from the peak positions are thought to represent the natural time scales during which intercluster proton motions are able to occur. The frequency shifts of the peak maxima with changing water concentration, although showing trends in some instances, do not exhibit a universal behavior for all EWs and do not correlate as well as the parameter n does with water concentration. Additionally, observed bimodal ϵ_{ac}'' curves strongly suggest the coexistence of two distinct types of hydrated clusters in these membranes. This is an interesting morphological issue that would be somewhat difficult to explore with conventional electron microscopic or small-angle X-ray scattering techniques.

Finally, we have generated Cole–Cole plots for these membranes in their dry sulfonic acid forms. The Cole–Cole distribution of relaxation times parameter (α) was extracted from well-defined depressed semicircles appearing in the high-frequency regime of the plots for the three membrane equivalent weights. We have suggested that α reflects the distribution of cluster sizes as well as, perhaps, the distribution of the manner in which the sulfonic acid-terminated side chains are packed within the clusters in the dry state.

In short, α and n are considered to be crude but useful indices of short- and long-range morphological regularity, respectively.

Eventually, organized comparisons should be made between dielectric relaxation spectra of short and long (e.g., Nafion) side chain perfluorosulfonic acid membranes. Meaningful comparisons will be possible when liberal amounts of samples of each side chain type are available over wide equivalent weight ranges. Owing to the fact that this availability was nonexistent at the time of our experimentation, we presently cannot offer a substantive discussion of this important issue. Meaningful comparisons will be made at such a time when it is possible to hold two of the variables, equivalent weight, sulfonic acid group number density, or water content, constant while the remaining quantity is varied. Of course, EW manipulations will affect the degree of TFE-like crystallinity, which in turn affects the equilibrium water uptake as well as other relevant membrane properties.

Acknowledgment. The financial support of the Dow Chemical Co., as well as valuable technical discussions with C. R. Martin (Dow), is gratefully acknowledged.

References and Notes

(1) Deng, Z. D.; Mauritz, K. A. *Macromolecules* **1992**, in press.
(2) Tant, M. R.; Darst, K. P.; Lee, K. D.; Martin, C. W. In *Multiphase Polymers: Blends and Ionomers*; Uktracki, L. A., Weiss, R. A., Eds.; ACS Symposium Series 395; American Chemical Society: Washington, DC, 1989; p 370.
(3) Moore, R. B.; Martin, C. R. *Macromolecules* **1989**, *22*, 3594.
(4) Freibert, F. J. M.S. Thesis: Infrared Spectroscopic Study of Aqueous Acidic Solutions Contained within the Nafion Ionomer Membrane; University of Southern Mississippi, 1989.
(5) Cole, K. S.; Cole, R. H. *J. Chem. Phys.* **1941**, *9*, 341.
(6) (a) Forsman, W. C. *Macromolecules* **1982**, *15*, 1032. (b) Forsman, W. C.; MacKnight, W. J.; Higgins, J. S. *Macromolecules* **1984**, *17*, 490.

Registry No. H_2O, 7732-18-5.